FULL PAPER

Dalton
www.rsc.org/dalton

Interaction of hydroperoxopalladium complexes, $(Tp^{R})(py)Pd–OOH$, with hydroxo-nickel and -cobalt complexes, $[(\mu\text{-}OH)(MTp^{R'})]_2$ (M = Ni, Co), leading to oxidative dehydrogenation of the saturated hydrocarbyl moiety in the ancillary ligand (Tp^{iPr2})†

Masato Kujime, Shiro Hikichi‡ and Munetaka Akita*

Chemical Resources Laboratory, Tokyo Institute of Technology, 4259 Nagatsuta, Midori-ku, Yokohama 226-8503, Japan. E-mail: makita@res.titech.ac.jp

Received 25th June 2003, Accepted 29th July 2003
First published as an Advance Article on the web 13th August 2003

Treatment of hydroperoxopalladium complexes, $(Tp^{R})(py)Pd–OOH$, with hydroxonickel complexes, $[(\mu\text{-}OH)NiTp^{R'}]_2$, when either Tp^{R} or $Tp^{R'}$ is Tp^{iPr2}, results in dehydrogenation of an isopropyl group of the Tp^{iPr2} ligand to give heterobimetallic di-μ-hydroxo complexes bearing the 3-isopropenyl-substituted Tp ligand $[HB(pz^{iPr2})_2(pz^{3\text{-isopropenyl-5-iPr}})$. Similar dehydrogenation is observed for the reaction with the hydroxocobalt complex bearing the Tp^{iPr2} ligand. The dehydrogenated products are characterized by spectroscopic and crystallographic methods and a mechanism involving a heterobimetallic μ-peroxo intermediate formed *via* dehydrative condensation has been proposed for the oxidative dehydrogenation.

Introduction

Dehydrative condensation of hydroxometal complexes (Scheme 1) is a versatile synthetic method for coordination compounds. Acidic substrates (H–A) are incorporated into the metal coordination sphere in the form of their conjugated bases. Because the eliminated water, the only byproduct, may fall out of the organic phase or can be readily removed by treatment with a drying agent, no further separation is needed to isolate the product. This method is useful for, in particular, synthesis of thermally unstable complexes.

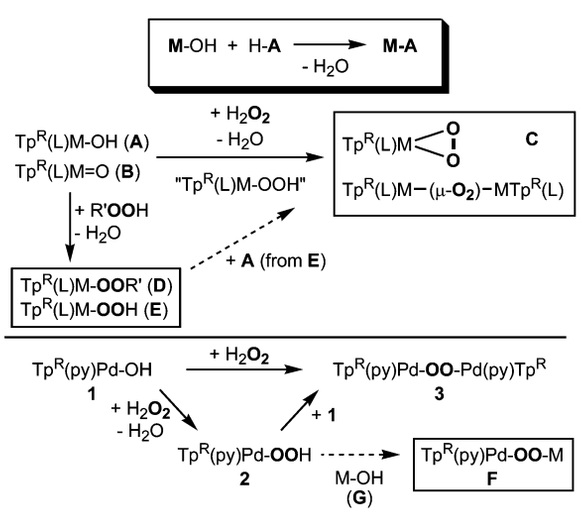

Scheme 1

We have employed this method for the systematic synthetic study of dioxygen complexes bearing hydrotris(pyrazolyl)-borato ligands (Tp^{R}).[1–3] As a result, a series of peroxo complexes **C** (dioxygen complexes) including thermally unstable derivatives has been obtained successfully by treatment of a hydroxo (**A**) or oxo complex (**B**) with H_2O_2 (Scheme 1).[4,5] Furthermore alkylperoxo complexes (M–OOR′ **D**) are prepared by similar dehydrative condensation of **A** with R′OOH.[6] These results suggest that a hydroperoxo species **E** is involved as an intermediate for the formation of the peroxo species **C** from **A**(**B**). Although hydroperoxo species **E** can, in principle, be accessible *via* dehydrative condensation of **A** with H_2O_2 in 1 : 1 ratio, resultant species **E** are usually too thermally unstable to be isolated and, therefore, the reaction pathway for the peroxo species had remained to be confirmed. During the course of our study, by using an isolated sample of the stable hydroperoxo complex, $Tp^{R}(py)Pd–OOH$ **2** (obtained from the hydroxo complex **1** and H_2O_2), we confirmed that the μ-peroxopalladium complex, $(\mu\text{-}O_2)[Pd(py)Tp^{R}]_2$ **3**, was formed following the sequence: **1** ⟶ **2** ⟶ **3**.[5]

The successful formation of the homometallic μ-peroxo complex **3** from **2** and **1** prompted us to examine the synthesis of a heterometallic derivative **F** *via* condensation of **2** with a hydroxo complex of a different metal (**G**) (Scheme 1). Compared to homometallic complexes heterometallic derivatives are rare due to the limited accessibility and, therefore, their chemistry has remained to be explored. Recently, the Cu,Fe μ-peroxo species has attracted much attention as the key intermediate of cytochrome c oxidase.[7] In a recent paper we reported the result of interaction of **3** with the hydroxocopper complex, $[(\mu\text{-}OH)CuTp^{iPr2}]_2$, in hope of formation of a heterobimetallic μ-peroxo species.[8] The interaction, however, resulted in the Cu-mediated redox decomposition of the Pd–OOH moiety *via* an outer sphere redox mechanism (not *via* a μ-peroxo intermediate) to give the cyclic alkylperoxopalladium complex resulting from C–H activation at a hydrocarbyl substituent in the Tp^{iPr2} ligand. Herein we wish to disclose the results of interaction of **2** with hydroxo complexes of nickel and cobalt, $[(\mu\text{-}OH)MTp^{R'}]_2$ **4** [M = Ni (**4(Ni)**), Co (**4(Co)**)],[9] leading to oxidative dehydrogenation of the hydrocarbyl moiety in the Tp^{iPr2} ligand.[3] The dehydrogenation process has been best interpreted in terms of a heterobimetallic μ-peroxo intermediate resulting from dehydrative condensation.

† Electronic supplementary information (ESI) available: Fig. 4: ^{1}H NMR monitoring of the reaction of $\mathbf{2}^{iPr2}$ and $\mathbf{4}^{iPr2}$**(Ni)** at −20 °C. See http://www.rsc.org/suppdata/dt/b3/b307262m/

‡ Present address: Department of Applied Chemistry, School of Engineering, University of Tokyo, Hongo, Bunkyo-ku, Tokyo 113-8656, Japan.

DOI: 10.1039/b307262m

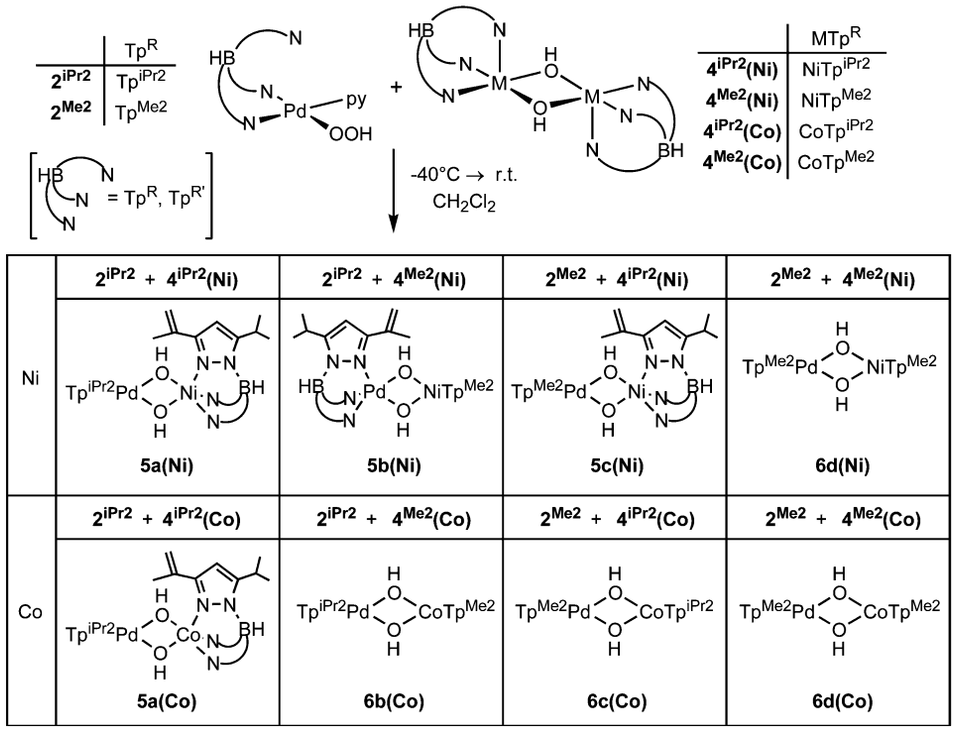

Scheme 2

Results and discussion

Interaction between 2 and 4: formation of heterometallic dehydrogenated (5) and non-dehydrogenated μ-hydroxo complexes (6).

The hydroperoxopalladium complex **2**[5a–c] was treated with the hydroxo complex **4**[9] in the presence of Na_2SO_4 (a dehydrating agent) at −40 °C and the resultant mixture was gradually warmed to room temperature (Scheme 2). No apparent color change was observed but spectroscopic and crystallographic analysis of the products showed conversion into two new types of the paramagnetic, heterobimetallic di-μ-hydroxo complexes depending on the Tp^R–$Tp^{R'}$–M combinations; complex **5** resulting from dehydrogenation of the 3-isopropyl group in the Tp^{iPr2} ligand and the non-dehydrogenated complex **6**. The reactions were so clean that the products were isolated by simple crystallization from MeCN. No significant amount of byproducts was isolated by further concentration and detected by spectroscopic methods (see below).

Spectroscopic characterization of heterometallic μ-hydroxo complexes 5 and 6

(i) IR: Formation of μ-hydroxo complexes. All products **5** and **6** exhibit IR features similar to those of the dinuclear di-μ-hydroxo complexes, [(μ-OH)MTp^R]$_2$ [M = Ni (**4(Ni)**), Co (**4(Co)**), Pd],[5d,9] which show the ν_{OH} and ν_{BH} vibrations (Table 1).

The OH vibrations suggest that the products **5** and **6** are not the desired μ-peroxo species (**F**) but hydroxo complexes analogous to **4**.

It is notable that complexes **5** and **6** show two ν_{BH} vibrations in the range of 2450–2550 cm^{-1}. In a previous paper, we reported that the ν_{BH} value was a useful indicator for the hapticity of the Tp^R ligand.[10] The ν_{BH} band for a κ^3-Tp^R ligand appears above 2500 cm^{-1}, whereas that for a κ^2-Tp^R ligand appears below 2500 cm^{-1}. As can be seen from Table 1, all products **5** and **6** show two ν_{BH} bands above and below 2500 cm^{-1}, indicating that the dinuclear complexes contain both κ^2-Tp^R and κ^3-Tp^R ligands. Because previous studies on the Tp^RM complexes[1] have revealed that the group 9 and 10 first row metal complexes (Co and Ni) and the palladium complexes adopt five- or six-coordinate structures with the κ^3-Tp^R ligand and four-coordinate square-pyramidal structure with the κ^2-Tp^R ligand, respectively,[4,5,11] complexes **5** and **6** should contain (κ^2-Tp^R)Pd and (κ^3-$Tp^{R'}$)Ni/Co fragments.

Table 1 Selected IR data for **5** and **6**[a]

Compound	ν_{OH}	ν_{BH}(κ^3-Tp^R)	ν_{BH}(κ^2-Tp^R)
5a(Ni)	3599	2535	2484
5b(Ni)	3651	2518	2479
5c(Ni)	3586	2537	2470
6d(Ni)	3627	2511	2472
5a(Co)	3601	2534	2483
6b(Co)	3649	2516	2476
6c(Co)	3652	2535	2475
6d(Co)	3558	2524	2475

[a] Observed as KBr pellets, reported in cm^{-1}.

In addition, the IR absorption observed for **2** around 1600 cm^{-1} disappears upon treatment with **4**. Because this absorption is associated with the pyridine ligand ($\nu_{C=N}$), the disappearance indicates loss of the pyridine ligand during the condensation. Thus the palladium center in **5** and **6** should be coordinated by the κ^2-Tp^R and two μ-OH ligands.

These IR features of **5** and **6** are consistent with the heterobimetallic di-μ-hydroxo complexes (κ^2-Tp^R)Pd(μ-OH)$_2$Ni/Co(κ^3-$Tp^{R'}$) with four-coordinate square-planar (Pd) and five coordinate square-pyramidal metal fragments (Ni/Co),

(ii) FD-MS: Occurrence of dehydrogenation. In order to confirm the dinuclear structure of the products **5** and **6** resulting from the condensation they were subjected to FD-MS analysis and the obtained spectra are shown in Fig. 1. The products **6d(Ni/Co)** obtained from the Tp^{Me2} complexes did not show any meaningful peaks.[13]

The agreement of the observed spectra with the spectra calculated for $Tp^RPd(\mu\text{-}OH)_2MTp^{R'}$ **6** supports the formation of the heterobimetallic di-μ-hydroxo complexes as suggested by the IR data. When the isotopic distribution is examined in detail, however, significant deviation from the values calculated

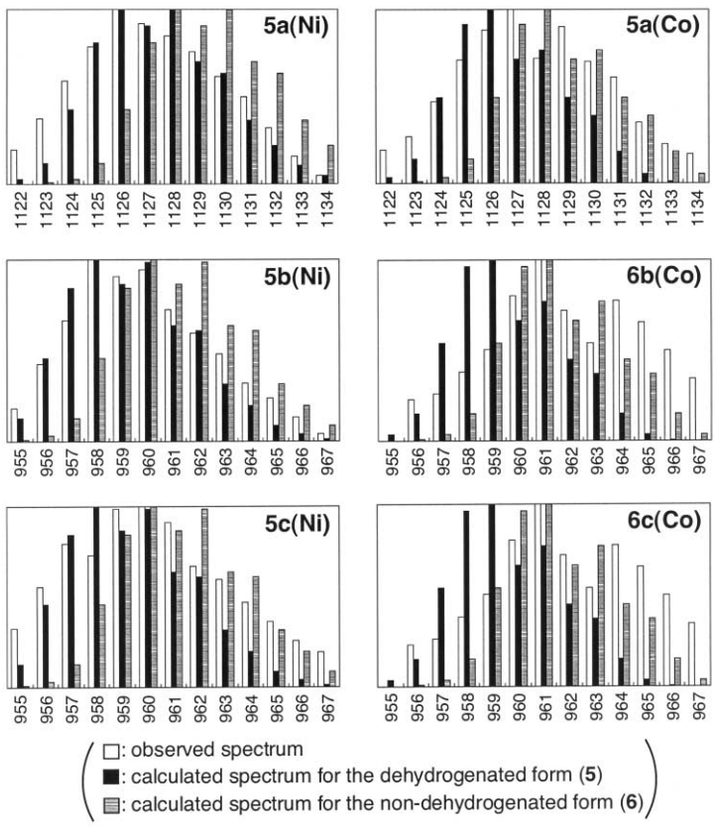

Fig. 1 FD-MS spectra for **5** and **6**.

for **6** is evident for complexes **5a(Ni)**, **5b(Ni)**, **5c(Ni)** and **5a(Co)**. The observed isotopic distribution for these products is found to be in good agreement with the patterns calculated for (**6** – 2H), suggesting the occurrence of a dehydrogenation process. Although the *m*/*z* values for **5** and the desired μ-peroxo species, $Tp^{R}Pd–O_2–MTp^{R'}$, are identical, the latter possibility has been eliminated by the above-mentioned IR data. In contrast to these complexes **5**, the composition of the other type of complexes [**6b**,**c(Co)**] has been confirmed to be the simple heterometallic di-μ-hydroxo complexes, $Tp^{R}Pd(\mu\text{-}OH)_2\text{-}MTp^{R'}$ **6**.

(iii) ^{1}H NMR: Symmetry of the dehydrogenated products 5. The paramagnetic products **5** and **6** give isotropically shifted ^{1}H NMR spectra. In Fig. 2, ^{1}H NMR spectra for the nickel complexes **5a**–**c(Ni)** are shown. Assignments of all signals are not always possible but the highly deshielded signals around 60 ppm have been assigned to the hydrogen atom at the 4-position of the pyrazolyl ring (4-pz-H)[3] of the $NiTp^{R}$ fragment by comparison with the ^{1}H NMR spectra of the starting compound **4(Ni)**. The appearance of the 4-pz-H signals in 1 : 2 ratio observed for **5a(Ni)** and **5c(Ni)** indicates that the Tp ligand coordinated to the nickel center (Tp^{iPr2}) is functionalized to give a mirror-symmetrical structure.[14] On the other hand, the 4-pz-H signal for **5b(Ni)** appears as a single resonance suggesting no change for the $NiTp^{Me2}$ part but functionalization of the other metal fragment ($PdTp^{iPr2}$). The Co-derivatives gave very widely shifted spectra, from which no structural information could be deduced.

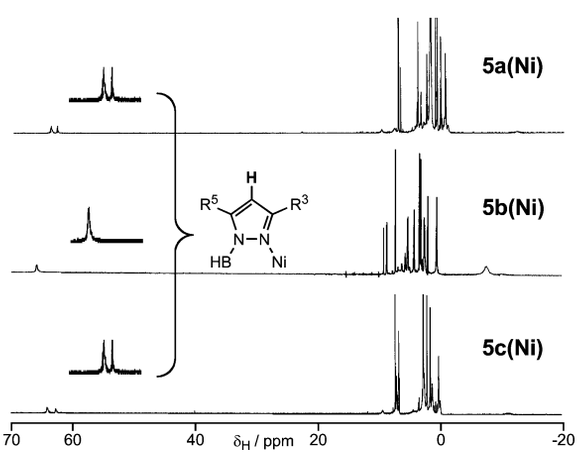

Fig. 2 ^{1}H NMR spectra of **5a(Ni)** (in C_6D_6), **5b(Ni)** (in $CDCl_3$) and **5c(Ni)** (in C_6D_6) observed at 200 MHz at 25 °C.

These ^{1}H NMR data for **5(Ni)** reveal that (1) the Tp^{iPr2} ligand is functionalized in a specific manner in preference to the Tp^{Me2} ligand, (2) the functionalization leads to a mirror-symmetrical structure, *i.e.* one of the three pyrazolyl rings in the Tp^{iPr2} ligand is functionalized, and (3) the 4-pz-H moieties in the $Tp^{R'}Ni$ unit are not functionalized.

Crystallographic characterization: dehydrogenation of the isopropyl group to give the isopropenyl group.

The spectroscopic features described above reveal that **5** is a heterobimetallic di-μ-hydroxo complex resulting from dehydrogenation of a pyrazolyl group in the Tp^{iPr2} ligand, and the site of the dehydrogenation has been confirmed by X-ray crystallography as compared with the non-dehydrogenated product **6**.

Molecular structures of **5a(Ni)**, **5b(Ni)**, **5c(Ni)**, **5a(Co)**, **6b(Co)** and **6c(Co)** have been determined by X-ray crystallography for single crystals obtained by recrystallization from MeCN. Their ORTEP views are shown in Fig. 3 and selected structural parameters are listed in Table 2. Complexes **5a(Ni)**·H_2O, **5a(Co)**·H_2O, **5b(Ni)**·MeCN and **6b(Ni)**·MeCN are characterized as the solvated forms.

As indicated by the spectroscopic characterization, the products **5** and **6** are determined as the heterobimetallic di-μ-hydroxo complexes. The palladium parts adopt four-coordinate

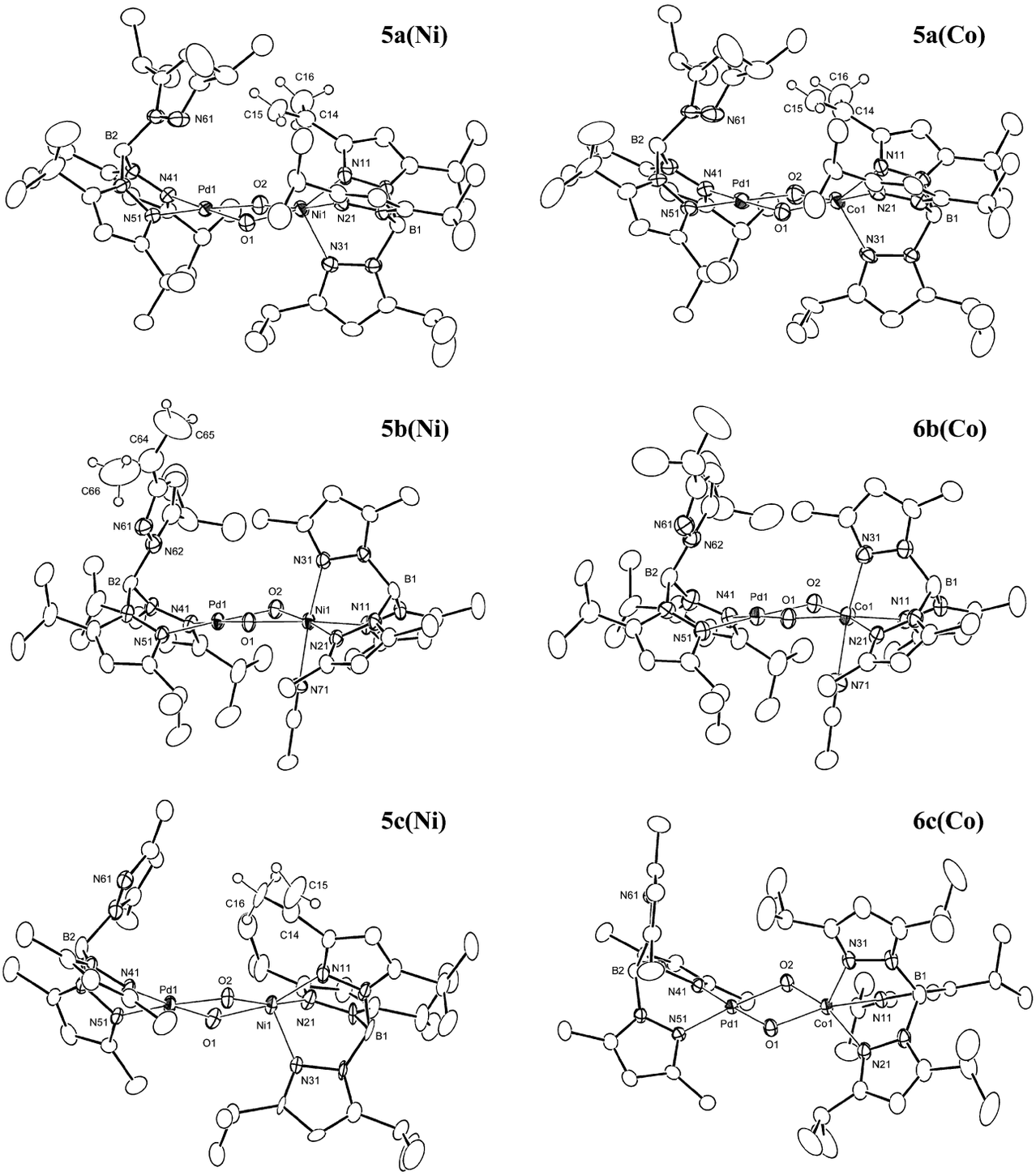

Fig. 3 Molecular structures of **5** and **6**. Thermal ellipsoids are drawn at the 30% probability level.

square-planar geometry with the κ^2-Tp^R and two μ-OH ligands. The κ^2-coordination is evident from (1) the Pd ··· N61 distances longer than 3.3 Å and (2) the orientation of the lone pair electrons of the N61 atoms, which are not directed to the palladium center. In the case of **5a(Ni)** and **5a(Co)**, a water molecule (omitted for clarity in Fig. 3) is incorporated between the O1 and N61 atoms through hydrogen bonding interactions [**5a(Ni)**: O1 ··· O3: 3.104(6); O3 ··· N61: 2.767(6) Å; **5a(Co)**: O1 ··· O3: 3.06(2); O3 ··· N61: 2.74(2) Å; O3: the oxygen atom of the water molecule]. As for the nickel/cobalt parts, a five-coordinate square-pyramidal geometry is observed for **5a(Ni)**, **5c(Ni)**, **5a(Co)** and **6c(Co)** derived from the hydroxo complexes with the Tp^{iPr2} ligand [$\mathbf{4}^{iPr2}$**(Ni)**, $\mathbf{4}^{iPr2}$**(Co)**], while, for the products derived from the less bulky, more Lewis-acidic Tp^{Me2} derivatives [**5b(Ni)**, **6b(Co)**], coordination of the MeCN solvate leads to a six-coordinate octahedral geometry. Although the τ values[15] calculated for the square-pyramidal parts [0.18: **5a(Ni)**; 0.05: **5c(Ni)**; 0.15: **5a(Co)**; 0.02: **6c(Co)**] indicate structures close to an ideal one, the chelating effect of the two bridging hydroxo ligands causes considerable distortion as is suggested by (1) the angles formed by the *trans*-basal ligands being as small as *ca.* 160° and (2) the puckered conformation of the Pd(μ-OH)$_2$M core. Although the Pd–O distances are anticipated to be longer than the M–O distances of the first row metal complexes, they turn out to be comparable (*ca.* 2.0 Å). This could be due to the four-coordinate palladium moiety being more Lewis acidic than the five- or six-coordinate nickel and cobalt moieties.

The site of dehydrogenation has been determined by X-ray crystallography to be an isopropyl group proximal to the metal

Table 2 Selected structural parameters for the core parts of **5** and **6**

Complex	**5a**(Ni)		**5b**(Ni)		**5c**(Ni)	
M	Ni	Pd	Ni	Pd	Ni	Pd
Bond lengths (Å)						
M–N11(N41)	2.039(3)	2.009(2)	2.105(4)	2.012(6)	2.070(9)	2.031(8)
M–N21(N51)	2.082(3)	2.014(3)	2.093(5)	2.004(4)	2.089(9)	2.006(9)
M–N31	2.037(3)	3.345(3)	2.109(5)	3.974(5)	2.013(9)	4.02(1)
M–N71	–	–	2.168(6)	–	–	–
M–O1	2.010(2)	2.017(2)	2.046(3)	1.998(5)	2.018(8)	2.022(7)
M–O2	2.030(2)	2.009(2)	2.068(5)	2.015(4)	2.045(7)	2.029(7)
Bond angles (°)						
N11(N41)–M–N21(N51)	87.3(1)	88.2(1)	89.8(2)	86.6(2)	86.5(4)	89.4(4)
N11–M–N31	90.9(1)	–	88.1(2)	–	92.4(4)	–
N21–M–N31	90.2(1)	–	86.4(2)	–	90.6(4)	–
N11(N41)–M–O1	159.5(1)	175.0(1)	171.3(2)	175.3(2)	164.2(3)	176.4(3)
N11(N41)–M–O2	90.5(1)	96.0(1)	95.0(2)	96.5(2)	95.5(3)	97.7(3)
N21(N51)–M–O1	100.3(1)	96.74(9)	96.4(2)	96.1(2)	96.0(3)	93.9(3)
N21(N51)–M–O2	170.3(1)	175.48(9)	173.5(2)	176.7(2)	167.5(3)	172.5(3)
N31–M–O1	107.9(1)	–	98.4(2)	–	103.2(3)	–
N31–M–O2	99.3(1)	–	98.2(2)	–	101.6(3)	–
O1–M–O2	78.78(9)	79.08(9)	78.4(2)	80.8(2)	78.9(3)	79.1(3)
Structural parameters for the isopropenyl and isopropyl parts[a]						
l_1	1.362(7)	[1.52]	1.36(3)	[1.52] [b]	1.41(3)	[1.50]
l_2	1.466(7)		1.42(2)		1.44(2)	
α	119.8(4)	[110.9]	119(1)	[111.3][b]	117(1)	[111.7]
β	116.4(4)		120(1)		118(1)	
γ	123.8(4)		121(2)		122(2)	
$\alpha + \beta + \gamma$	360.0	[332.7]	360	[333.9][b]	357	[335.1]
θ	33.5(6)		15(1)		29(1)	
χ		[66 (47–90)][c]		[69 (47–82)][b,c]		[61 (44–80)][c]

Complex	**5a**(Co)		**6b**(Co)		**6c**(Co)	
M	Co	Pd	Co	Pd	Co	Pd
Bond lengths (Å)						
M–N11(N41)	2.087(6)	1.989(5)	2.139(6)	2.016(9)	2.140(2)	2.001(2)
M–N21(N51)	2.114(5)	2.011(6)	2.126(8)	1.991(6)	2.141(3)	2.011(3)
M–N31	2.067(6)	3.300(7)	2.145(9)	3.867(8)	2.073(3)	4.350(3)
M–N71	–	–	2.236(9)	–	–	–
M–O1	2.024(5)	2.020(4)	2.020(5)	2.010(7)	2.011(3)	2.006(2)
M–O2	2.046(5)	2.009(5)	2.080(7)	2.001(5)	2.019(3)	2.004(3)
Bond angles (°)						
N11(N41)–M–N21(N51)	85.8(2)	88.3(2)	88.7(3)	86.7(3)	84.4(1)	87.8(1)
N11–M–N31	89.0(2)	–	86.5(3)	–	89.6(1)	–
N21–M–N31	89.1(2)	–	85.4(3)	–	88.8(1)	–
N11(N41)–M–O1	157.6(2)	174.9(2)	170.9(3)	174.7(2)	159.3(1)	174.0(1)
N11(N41)–M–O2	90.1(2)	95.1(2)	95.1(3)	96.2(3)	94.25(9)	96.9(1)
N21(N51)–M–O1	100.5(2)	96.8(2)	97.3(2)	96.6(3)	97.3(1)	97.6(1)
N21(N51)–M–O2	166.7(2)	176.6(2)	173.5(2)	176.6(3)	160.2(1)	175.1(1)
N31–M–O1	112.5(2)	–	100.8(2)	–	111.0(1)	–
N31–M–O2	103.5(2)	–	100.1(3)	–	110.9(1)	–
O1–M–O2	78.9(2)	79.9(2)		80.5(2)	77.2(1)	77.6(1)
Structural parameters for the isopropenyl and isopropyl parts [a]						
l_1	1.35(1)	[1.52]	[1.51] [b]		[1.50]	
l_2	1.49(1)					
α	122.9(8)	[110.8]	[111.2] [b]		[111.7]	
β	113.5(8)					
γ	123.3(8)					
$\alpha + \beta + \gamma$	359.7	[332.3]	[333.7] [b]		[335.1]	
θ	37(1)					
χ		[67 (51–89)] [c]		[62 (45–81)][b,c]		[67 (55–83)] [c]

[a] The values in brackets are averaged values for the non-dehydrogenated isopropyl groups. [b] The disordered part is not included. [c] Averaged value. Numbers in parentheses are distributions.

center (3-position), which is converted to the isopropenyl group. In Table 2 structural parameters for the isopropenyl part is compared with the non-dehydrogenated isopropyl groups (shown in square brackets). The formation of the isopropenyl group has been confirmed by the two structural features: (1) the C–C lengths (l_1 and l_2) and (2) planarity of the central carbon atom. The olefinic C=C distance (l_1 of *ca.* 1.36 Å) is substantially shorter than the aliphatic C–C distance (l_2 of *ca.* 1.47 Å) and they are comparable to the typical C(sp^2)=C(sp^2) (1.32 Å) and C(sp^2)–C(sp^3) lengths (1.51 Å), respectively.[16,17] The C=C distances are also shorter than the C(sp^3)–C(sp^3) lengths of the non-dehydrogenated isopropyl groups (>1.50 Å) shown in square brackets. The sum of the bond angles ($\alpha + \beta + \gamma$), which is in the range of 357–360°, also supports the planar sp^2-hybridization of the central carbon atom resulting from dehydrogenation. In this case, too, the sum is substantially larger than that for the non-dehydrogenated isopropyl group with the sp^3-hybridized carbon atom (332–335°). Furthermore it is notable that the formed alkenyl functional group tends to be coplanar with the pyrazolyl ring so as to be conjugated with the aromatic π-system as is evident from the small dihedral angles formed by the pz plane and the isopropenyl olefin plane (θ 17–38°; Table 2). The situation is in contrast to that of the isopropyl groups, where the methyl groups are arranged so as to minimize the steric repulsion with the pz ring. The situation is apparent from the large dihedral angle χ defined by the pz plane and a plane perpendicular to the methine C–H vector (61–69°; Table 2).

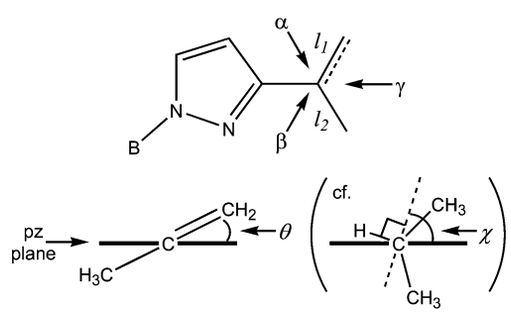

Reaction mechanism

(i) Attempts to detect intermediates. The dehydrative condensation between the hydroperoxopalladium complex **2** and the dinuclear di-μ-hydroxo complex **4** is expected to form a heterobimetallic μ-peroxo intermediate **F**. We tried to detect the intermediate by spectroscopic monitoring (^{1}H NMR, UV-vis) of the reaction mixture at low temperatures but such attempts were unsuccessful. As an example, the result of ^{1}H NMR monitoring of the reaction of $\mathbf{2}^{\mathbf{iPr2}}$ and $\mathbf{4}^{\mathbf{iPr2}}$**(Ni)** at −20 °C is shown as ESI.† The gradual conversion of the starting compounds into the products was observed during the reaction course over 2 h but neither intermediate nor byproduct could be detected, indicating that the initial condensation process, in which **2** and **4** were consumed at the same time, was the rate-determining step. The ^{1}H NMR analysis reveals that the dehydrative condensation and the successive reactions are quite selective and the formation of **5a(Ni)** is virtually quantitative. Any transient intermediate could not be detected by UV-vis monitoring a reaction mixture from −80 °C to ambient temperature. We also examined the interactions of the Tp^{Me2} and Tp^{Me3} derivatives, which should be resistant to homolytic hydrogen abstraction (see below). However, in this case, too, no intermediate could be detected.

(ii) Plausible reaction mechanism. The structural features observed for **5** and **6**, combined with the results of the spectroscopic characterization, reveal that the site of the dehydrogenation is an isopropyl group proximal to the metal center (3-position). It should be noted that, for **5b(Ni)** and **5c(Ni)**, the isopropyl group in the Tp^{iPr2} ligand containing the tertiary methine group is dehydrogenated in preference to the methyl substituent in Tp^{Me2}, suggesting viability of a radical intermediate. Tertiary radical species resulting from H-abstraction from the methine C–H moiety are more stable than secondary and primary alkyl radicals. A similar trend of the reactivity order has been noted for peroxo complexes. As a typical example, the dinuclear bis-μ-oxo complexes, $[(\mu\text{-O})MTp^R]_2$ **7** (M = Ni, Co), can be raised.[4] The Tp^{iPr2} derivatives are found to be too reactive to be characterized and they undergo abstraction of the methine hydrogen atom of a 3-isopropyl group in the Tp^{iPr2} ligand even at low temperatures to give ligand-oxygenated products. However, replacement of the isopropyl substituents by the methyl substituents ($Tp^{iPr2} \longrightarrow Tp^{Me2}$, Tp^{Me3}) leads to the successful isolation and full characterization of the bis-μ-oxo complexes, although slow decomposition causing oxygenation of the 3-methyl substituent is observed. Dehydrogenation of the 3-isopropyl substituent of the $Tp^{iPr,Me}$ ligand was noted for a derivative of the bis-μ-oxo species, $[(\mu\text{-O})\text{-}CoTp^{iPr,Me}]_2$, by Reinaud and Theopold.[18]

On the basis of the structures of the reaction products and the previously obtained results on the $Tp^RM\text{–}O_2$ adducts,[1] a plausible mechanism for the reaction between **2** and **4** is proposed as summarized in Scheme 3. The first step should be dehydrative condensation producing a heterobimetallic μ-peroxo species **F**. We reported preparation of homometallic μ-peroxo species [M = Pd (**3**)] and the related bis-μ-oxo species [M = Ni, Co (**7**)] *via* this synthetic method.[4,5] Subsequent O–O homolysis should give two types of metaloxy radicals (**H**), which abstract hydrogen atoms from a proximal 3-isopropyl substituent of the Tp^{iPr2} ligand (**I**; As a typical example, an intermediate for oxygenation of the Tp^{iPr2}Ni part is shown.) to give the isopropenyl group. The μ-η^2:η^2-form **F′** and the bis-μ-oxo form **H′** resulting from loss of the pyridine ligand could be alternative intermediates but they could be excluded, because stabilization by electron donation from the metal centers (**H″**) as observed for the bis-μ-oxo complexes of nickel(III) and cobalt(III) (**7**)[4] is not feasible for the palladium species. No Pd(III) species has been detected in the Tp^RPd chemistry.[5] The ligand oxygenation of alkylperoxo (**8**) and bis-μ-oxo complexes of cobalt and nickel (**7**) has been interpreted in terms of oxyl radical intermediates resulting from O–O bond homolysis (**J**, **K** ⟶ **L**).[4]

As for the non-dehydrogenated heterobimetallic di-μ-hydroxo complex **6**, there is a possibility that **6** may be formed by interaction of **4** with the hydroxopalladium complex **1**, which may result from decomposition of **2**.[19] This possibility has been excluded by the reaction of isolated samples of **1** and **4**, which resulted in recovery of the starting complexes (Scheme 4). This result suggests that even the non-dehydrogenated products **6** are formed *via* dinuclear intermediates, most likely the μ-peroxo intermediates **F**.

It should be noted that (1) the μ-peroxodipalladium complex **3** is stable with respect to O–O homolysis and instead (2) the Pd–O bond is susceptible to heterolysis to undergo nucleophilic attack of the resultant $Pd\text{–}O_2^-$ species. Thus the reactivity of the μ-peroxo species is highly affected by the metal component attached to it and the high reactivity of the Pd–Ni/Co μ-peroxo intermediates **F** are in sharp contrast to the remarkably stable μ-peroxodipalladium complex **3**, which decomposes at room temperature over the course of >1 day. Let us point out intriguing reaction aspects of the present system. First, of the two Tp^{iPr2} ligands in **5a(Ni)** and **5a(Co)**, the Tp^{iPr2}Ni/Co part is oxidized in preference to the Tp^{iPr2}Pd part. Secondly, as for the combinations of $\mathbf{2}^{\mathbf{Me2}}$ + $\mathbf{4}^{\mathbf{iPr2}}$ and $\mathbf{2}^{\mathbf{iPr2}}$ + $\mathbf{4}^{\mathbf{Me2}}$, dehydrogenation is observed only for the nickel complexes **5b(Ni)** and **5c(Ni)** and the cobalt systems afford the non-dehydrogenated products **6b(Co)** and **6c(Co)**. At the moment we do not have any evidence, which can account for these differences. Because the dehydrogenation is observed for both of the Ni (**5a(Ni)**) and Co

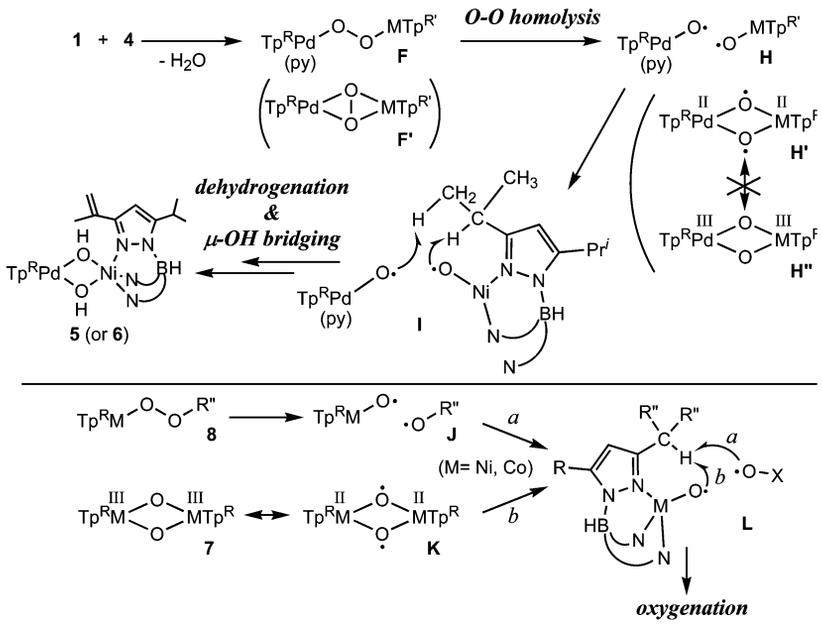

Scheme 3

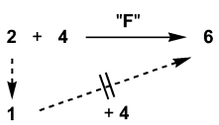

Scheme 4

systems (**5a(Co)**), the reactivity of the metaloxy intermediates **I** may be similar. Thus the difference observed for the **b** and **c** series could be ascribed to the subtle difference in the arrangement of the oxyl radical with respect to the methine C–H bond to be abstracted.

Interaction of the heterobimetallic di-μ-hydoxo complexes 5 and 6 with H_2O_2

Finally, isolated samples of **5** and **6** were further subjected to condensation with H_2O_2 (excess), which might afford μ-peroxo species (Scheme 5). The reaction mixtures were analyzed by FD-MS spectroscopy, because the reactions afforded rather complicated mixtures, from which pure samples could not be isolated. The reaction of the propenyl-nickel complex **5a(Ni)** gave a spectrum containing the parent peak for the dinuclear μ-enolato complex **9**, which was previously obtained by spontaneous decomposition of the bis-μ-oxo complex $\mathbf{7}^{\mathbf{iPr2}}$ (in situ generated from $\mathbf{4}^{\mathbf{iPr2}}$) in the presence of an excess amount of H_2O_2.[4d] The identity was further supported by the IR absorption (1617 cm^{-1}) observed for both the reaction mixture and **9**, which should be ascribed to the C=C vibration of the enolate part. This result suggests that the formation process of the enolate complex **9** from $\mathbf{7}^{\mathbf{iPr2}}$ involves dehydrogenation to give the propenyl group (as in **5**) followed by oxygenation of the resultant olefinic group. Taking into account the formation of **9**, the peaks around 1124 cm^{-1} were attributed to the heterobimetallic complex **10** containing the same partial structure as that of **9** (the enolate group). The reaction of **6b(Co)** gave the mass peaks corresponding to **6b(Co)** + 14*n* (*n* = 1–3) (Scheme 3). The regular increase of the mass number by 14 [O (16) − 2H (2)] suggests occurrence of a dehydrogenative oxygenation process. Dehydrogenation of the isopropyl group followed by epoxidation of the resultant isopropenyl group is a possible process but no other experimental support has been obtained. The transformation was repeated up to three times in accordance with the number of the 3-propyl groups proximal to the metal center in the Tp^{iPr2} ligand. Mass spectra for the other reactions revealed recovery of the starting complexes and no evidence for oxygenation was obtained.

Conclusions

The interaction of the hydroperoxopalladium complex **2** with the hydroxo complexes of nickel and cobalt **4** produces the heterobimetallic di-μ-hydroxo complexes **5** and **6**. Complex **5** contains the 3-isopropenyl substituted Tp ligand [$HB(pz^{3\text{-isopropenyl-5-iPr}})pz^{iPr2}_2$] resulting from oxidative dehydrogenation of a 3-isopropyl group of the Tp^{iPr2} ligand, whereas the Tp^{iPr2} ligand in **6** remains unaffected, as revealed by spectroscopic and crystallographic analyses. Key features of the present system are as follows. (1) The Tp^{iPr2} ligand is dehydrogenated specifically in preference to the Tp^{Me2} ligand. (2) Tp^{iPr2}Ni complexes are dehydrogenated, whereas dehydrogenation of the cobalt system is observed only for the Tp^{iPr2}Pd/$CoTp^{iPr2}$ combination. On the basis of the feature (1) and the previous results on the related $Tp^{R}M–O_2$ chemistry a heterobimetallic μ-peroxo intermediate **F** has been proposed and the oxyl radical species **I** resulting from O–O bond homolysis should abstract the methine C–H hydrogen atom to cause the dehydrogenation.

Combined with the previous results it has been revealed that isopropyl-substituted Tp ligands are susceptible to several types of oxidative transformations mediated by oxyl radical intermediates (Scheme 6), which are derived from peroxo species of various coordination structures. It is remarkable that all transformations shown in Scheme 6 involve C–H activation of the isopropyl group. Further studies on the metal–peroxo species should lead to development of catalytic functionalization processes of hydrocarbons.

Experimental

All manipulations were carried out using Schlenk tube technique. CH_2Cl_2 (P_4O_{10}) and MeCN (CaH_2) were treated with appropriate drying agents, distilled, and stored under argon. IR (measured as KBr pellets; reported in cm^{-1}) and FD-MS spectra were obtained on a JASCO FT/IR 5300 and JEOL JMS–700 spectrometer, respectively. ^1H NMR spectra were recorded on Bruker AC200 (200 MHz) and JEOL EX-400 spectrometers (400 MHz; variable temperature measurements). Deuterated solvents for NMR measurements containing 0.5% TMS were dried over molecular sieves and distilled under

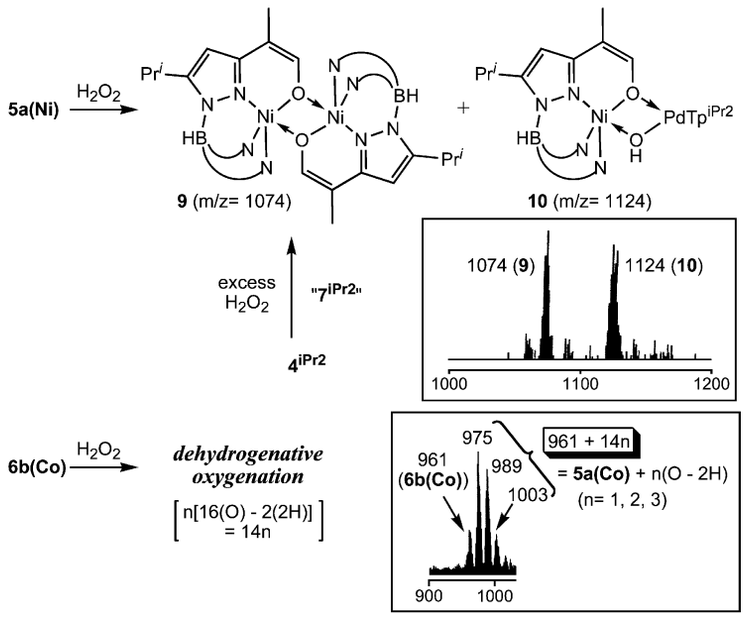

Scheme 5

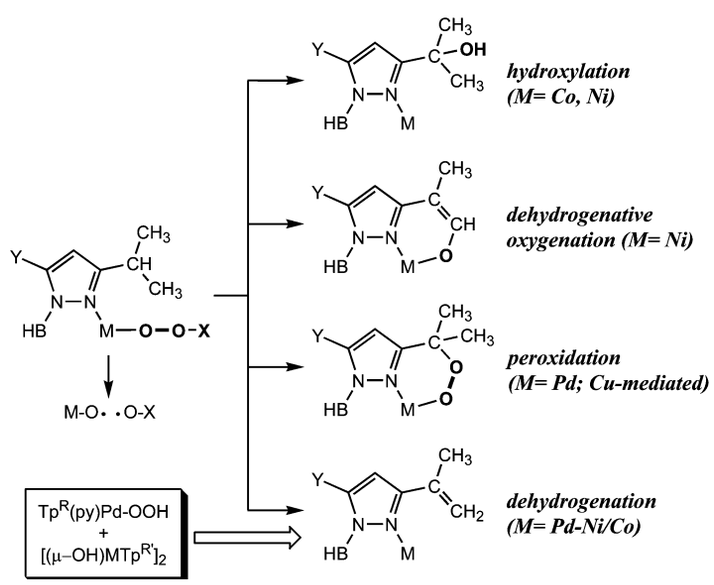

Scheme 6

reduced pressure. UV-vis monitoring at low temperatures were carried out using a Multi Channel Spectrometer (Fastevert S-2400, Soma Optics Ltd.) equipped with a Quartz Immersion Probe for low temperatures (Hellma, 661–202-UV). Starting complexes **2**[5d] and **4**[9] were prepared according to the procedures reported in our previous paper. Complex **2**^{Me2} was prepared in 32% yield in a manner as described for the Tp^{iPr2} derivative **2**^{iPr2}.[5c] ^{1}H NMR ($CDCl_3$) δ_H 8.58 (2H, d, J = 6 Hz, *o*-py), 7.77 (1H, t, J = 8 Hz, *p*-py), 7.29 (2H, t, J = 7 Hz, *m*-py), 5.86, 5.78, 5.68 (1H × 3, s, 4-pz-H), 2.46, 2.42, 2.39, 2.12, 2.08, 1.56 (3H × 6, s, Me). IR (KBr) 2513 (ν_{BH}), 1605 cm^{-1} (py).

Interaction between 2 and 4: formation of 5 and 6

As a typical example, the experimental procedure for the reaction between **2**^{iPr2} and **4**^{iPr2}**(Ni)** is described below. To a CH_2Cl_2 solution (10 mL) of **2**^{iPr2} (112 mg, 0.164 mmol) was added Na_2SO_4 (ca. 100 mg) and the mixture was cooled to −40 °C. A CH_2Cl_2 solution (10 mL) of **4**^{iPr2}**(Ni)** (61 mg, 0.082 mmol) was added dropwise and the resultant mixture was gradually warmed to room temperature. Filtration through a Celite pad followed by evaporation under reduced pressure and crystallization from MeCN gave **5a(Ni)** as green crystals (87 mg, 0.077 mmol, 53% yield). Anal. Calc. For $C_{54}H_{92}N_{12}O_2B_2NiPd$: C, 57.49; H, 8.22; N, 14.90. Found: C, 57.13; H, 7.86; N, 14.98%. Other reactions were carried out as described for **5a(Ni)**. The color of the nickel and cobalt complexes were green and red purple, respectively. **5b(Ni)**: 58% yield. Anal. Calc. for $C_{42}H_{68}N_{12}O_2B_2NiPd$: C, 52.56; H, 7.14; N, 17.51. Found: C, 51.73; H, 6.92; N, 17.20. **5c(Ni)**: 46% yield. Anal. Calc. for $C_{42}H_{68}N_{12}O_2B_2NiPd$: C, 52.56; H, 7.14; N, 17.51. Found: C, 52.48; H, 7.37; N, 17.30. **5a(Co)**: 53% yield. Anal. Calc. for $C_{54}H_{92}N_{12}O_2B_2CoPd$: C, 57.48; H, 8.22; N, 14.90. Found: C, 57.04; H, 8.04; N, 14.67. **6b(Co)**: 45% yield. Anal. Calc. for $C_{42}H_{68}N_{12}O_2B_2CoPd$: C, 52.43; H, 7.33; N, 17.47. Found: C, 51.84; H, 7.07; N, 17.27. **6c(Co)**: 44% yield. Anal. Calc. for $C_{42}H_{68}N_{12}O_2B_2CoPd$: C, 52.43; H, 7.33; N, 17.47. Found: C, 52.16; H, 7.05; N, 17.25%. Despite several attempts analytically pure samples of **6d(Ni)** and **6d(Co)** could not be obtained.[13]

X-Ray crystallography

Crystallographic data are summarized in Table 3. Single crystals of **5a(Ni)**·H_2O, **5b(Ni)**·MeCN, **5c(Ni)**, **5a(Co)**·H_2O,

Table 3 Crystallographic data

Complex	**5a(Ni)**·H_2O	**5b(Ni)**·MeCN	**5c(Ni)**	**5a(Co)**·H_2O	**6b(Co)**·MeCN	**6c(Co)**
Formula	$C_{62}H_{106}N_{16}O_3B_2$-NiPd	$C_{50}H_{80}N_{16}O_2B_2$-NiPd	$C_{46}H_{74}N_{14}O_2B_2$-NiPd	$C_{62}H_{106}N_{16}O_3B_2$-CoPd	$C_{50}H_{82}N_{16}O_2B_2$-CoPd	$C_{51}H_{83.5}N_{16.5}O_2B_2$-CoPd
Solvates	4MeCN	3MeCN	2MeCN	4MeCN	3MeCN	3.5MeCN
M_r	1310.34	1124.01	1041.90	1310.34	1126.26	1146.78
Crystal system	Monoclinic	Triclinic	Monoclinic	Monoclinic	Triclinic	Triclinic
Space group	$P2_1/c$	$P\bar{1}$	$P2_1/n$	$P2_1/c$	$P\bar{1}$	$P\bar{1}$
a/Å	15.8998(4)	13.254(1)	22.458(3)	15.840(1)	13.324(3)	13.356(1)
b/Å	23.5702(8)	21.125(2)	9.007(1)	23.393(2)	20.964(5)	21.0836(8)
c/Å	20.0482(6)	12.1299(8)	26.689(4)	20.111(1)	12.165(2)	12.1174(9)
α/°	90	101.662(4)	90	90	101.75(1)	95.350(4)
β/°	104.810(1)	112.767(3)	94.160(2)	104.604(3)	112.935(6)	114.865(1)
γ/°	90	89.006(5)	90	90	88.301(8)	84.508(4)
V/Å^3	7263.7(4)	3060.0(4)	5384(1)	7211.6(8)	3059(1)	3076.3(3)
Z	4	2	4	4	2	2
D_c/g cm^{-3}	1.198	1.220	1.285	1.207	1.223	1.238
μ/mm^{-1}	0.558	0.650	0.733	0.531	0.614	0.612
No. of reflections	52663	22208	11219	38840	15957	24065
No. of variables	778	657	612	733	631	691
$R1$ ($I > 2\sigma(I)$)	0.0647	0.0786	0.0928	0.0846	0.0886	0.0551
No. data	12893	8286	3583	6077	4652	11043
$wR2$ (all data)	0.1865	0.2083	0.2352	0.2218	0.2198	0.1552
No. data	15842	12561	7556	15107	10718	12688

6b(Co)·MeCN, and **6c** were obtained by recrystallization from MeCN and mounted on glass fibers.

Diffraction measurements were made on a Rigaku RAXIS IV imaging plate area detector with Mo-Kα radiation (λ = 0.71069 Å) at −60 °C. Indexing was performed from two oscillation images, which were exposed for 5 min. The crystal-to-detector distance was 110 mm ($2\theta_{max}$ = 55°). Neutral scattering factors were obtained from the standard source. In the reduction of data, Lorentz and polarization corrections and empirical absorption corrections were made.[20] Crystallographic data and results of structure refinements are listed in Table 3.

The structural analysis was performed on an IRIS O2 computer using teXsan structure solving program system obtained from the Rigaku Corp., Tokyo, Japan.[21] Neutral scattering factors were obtained from the standard source.[22]

The structures were solved by a combination of the direct methods (SHELXS-86)[23] and Fourier synthesis (DIRDIF94).[24] Least-squares refinements were carried out using SHELXL-97[23] (refined on F^2) linked to teXsan. Unless otherwise stated all non-hydrogen atoms were refined anisotropically and methyl hydrogen atoms of the Tp^{iPr2} ligand were refined using riding models and other hydrogen atoms were fixed at the calculated positions. The methylene hydrogen atoms of the dehydrogenated isopropenyl moieties were refined using riding models. Details of the refinements were as follows. **5a(Ni)**: One of the MeCN solvates was found to be disordered (N74 : N75 = 0.5 : 0.5). The OH hydrogen atoms, one of hydrogen atoms attached to the water molecule (O3) and methyl hydrogen atoms attached to the MeCN solvates were fixed at the final stage of the refinement. **5b(Ni)**: During the refinement one of the isopropyl groups was found to be disordered and refined taking into account two components (C48,49 : C48a,49a = 0.63 : 0.37). Hydrogen atoms were fixed at the final stage of the refinement and hydrogen atoms attached to the disordered part were not included in the refinement. **5c(Ni)**: The methylene hydrogen atoms of the isopropenyl moiety (H5,6) were refined isotropically. Hydrogen atoms attached to one of the MeCN solvates (highly disordered) were not included in the refinement and other MeCN hydrogen atoms were fixed at the final stage of the refinement. The OH hydrogen atoms were not included in the refinement. **5a(Co)**: The MeCN solvates were refined isotropically and one of them was found to be disordered and refined with two components (N74 : N75 = 0.5 :0.5). The OH hydrogen atoms and methyl hydrogen atoms attached to the MeCN solvates were fixed at the final stage of the refinement. Hydrogen atoms attached to the hydroxo ligands, the water molecule (O3) and the disordered MeCN molecule were not included in the refinement. **6b(Co)**: During the refinement one of the isopropyl groups was found to be disordered and refined taking into account two components (C47,48,49 : C47a,48a,49a = 0.63 : 0.37; refined isotropically). The OH hydrogen atoms were refined isotropically and the other hydrogen atoms were fixed at the final stage of the refinement. Hydrogen atoms attached to the disordered part were not included in the refinement. **6c(Co)**: The OH hydrogen atoms, which were associated with one of the disordered MeCN molecule, were not included and the methyl hydrogen atoms attached to the MeCN molecules were fixed at the final stage of the refinement.

CCDC reference numbers 198038 and 213612–213636.

See http://www.rsc.org/suppdata/dt/b3/b307262m/ for crystallographic data in CIF or other electronic format.

Acknowledgements

We are grateful to the Ministry of Education, Culture, Sports, Science and Technology of the Japanese Government for financial support of this research (Grant-in-Aid for Scientific Research on Priority Areas: 11228201).

References

1 M. Akita and S. Hikichi, *Bull. Chem. Soc. Jpn.*, 2002, **75**, 1657.
2 S. Trofimenko, *Scorpionates The Coordination Chemistry of Polypyrazolylborate Ligands*, Imperial College Press, London, 1999.
3 Abbreviations used in this paper: Tp^R, $Tp^{R'}$: hydrotris(pyrazolyl)-borato ligands; Tp^{iPr2}: the 3,5-diisopropylpyrazolyl derivative; Tp^{Me2}: 3,5-dimethylpyrazolyl derivative; Tp^{Me3}: 3,4,5-trimethylpyrazolyl derivative; pz^R: pyrazolyl group; 4-pz-H: the hydrogen atom at the 4-position of the pz^R group.
4 (*a*) S. Hikichi, H. Komatsuzaki, N. Kitajima, M. Akita, M. Mukai, T. Kitagawa and Y. Moro-oka, *Inorg. Chem.*, 1997, **36**, 266; (*b*) S. Hikichi, M. Yoshizawa, Y. Sasakura, M. Akita and Y. Moro-oka, *J. Am. Chem. Soc.*, 1998, **120**, 10567; (*c*) S. Hikichi, M. Yoshizawa, Y. Sasakura, H. Komatsuzaki, M. Akita and Y. Moro-oka, *Chem. Lett.*, 1999, 979; (*d*) S. Hikichi, M. Yoshizawa, Y. Sasakura, H. Komatsuzaki, Y. Moro-oka and M. Akita, *Chem.–Eur. J.*, 2001, **7**, 5011; (*e*) S. Hikichi, Y. Sasakura, M. Yoshizawa, Y. Ohzu, Y. Moro-oka and M. Akita, *Bull. Chem. Soc. Jpn.*, 2002, **75**, 1255.
5 (*a*) M. Akita, T. Miyaji, S. Hikichi and Y. Moro-oka, *Chem. Commun.*, 1998, 1005; (*b*) M. Akita, T. Miyaji, S. Hikichi and Y. Moro-oka, *Chem. Lett.*, 1999, 813; (*c*) T. Miyaji, M. Kujime, S. Hikichi, Y. Moro-oka and M. Akita, *Inorg. Chem.*, 2002, **41**, 5286; (*d*) M. Akita, T. Miyaji, N. Muroga, C. Mock-Knoblauch, S. Hikichi, W. Adam and Y. Moro-oka, *Inorg. Chem.*, 2000, **39**, 2096.

6 Co complex: S. Hikichi, H. Komatsuzaki, M. Akita and Y. Moro-oka, *J. Am. Chem. Soc.*, 1998, **120**, 4699; Pd complex: ref. 5. For other metal complexes, see ref. 1.
7 S. Ferguson-Miller and G. T. Babcock, *Chem. Rev.*, 1996, **96**, 2889; T. Chishiro, Y. Shimazaki, F. Tani, Y. Tachi, Y. Naruta, S. Karasawa, S. Hayami and Y. Maeda, *Angew. Chem., Int. Ed.*, 2003, **42**, 2788.
8 M. Kujime, S. Hikichi and M. Akita, *Chem. Lett.*, 2003, **32**, 486.
9 N. Kitajima, S. Hikichi, M. Tanaka and Y. Moro-oka, *J. Am. Chem. Soc.*, 1993, **115**, 5496.
10 M. Akita, K. Ohta, Y. Takahashi, S. Hikichi and Y. Moro-oka, *Organometallics*, 1997, **16**, 4121.
11 According to the CSD database, of the 73 Tp^{R}Ni/Co complexes listed therein only two complexes contain a κ^2-Tp^{R} ligand and the others are κ^3-Tp^{R} (70 examples) and κ^1-Tp^{R} complexes (1 example).[12a,b] On the other hand, 20 of the 22 Tp^{R}Pd complexes contain a κ^2-Tp^{R} ligand and a κ^3-Tp^{R} coordination has been found for only three examples.[12c].
12 (*a*) κ^1- and κ^2-Tp^{R}Ni complexes: E. Gutierrez, S. A. Hudson, A. Monge, M. C. Nicasio, M. Paneque and C. Ruiz, *J. Organomet. Chem.*, 1998, **551**, 215; (*b*) N. Shirasawa, T. T. Nguyet, S. Hikichi, Y. Moro-oka and M. Akita, *Organometallics*, 2001, **20**, 3582; (*c*) M. Kujime, S. Hikichi and M. Akita, *Organometallics*, 2001, **20**, 4049; see also ref. 5d.
13 Complexes **6d(Ni/Co)** could not be characterized satisfactorily. ESI- and FAB-MS also did not provide useful information. Single crystals and satisfactory elemental analyses were not obtained despite several attempts. Their characterization as **6** was based on the their IR spectra, which were virtually a superposition of those of the two hydroxo complexes $[(\mu\text{-OH})PdTp^{Me2}]_2$ and **4^{Me2}(Ni/Co)**, suggesting no structural change for the Tp^{Me2} ligands.
14 The Tp^{R} ligand in four- or five-coordinate complexes is usually fluxional *via* intramolecular rearrangement of the three pyrazolyl rings, which are observed equivalent at higher temperature (NMR). So even if one of the Tp^{R}M fragments in a dinuclear complex becomes unsymmetrical (mirror-symmetrical), the other non-functionalized Tp^{R}M fragment shows a single set of the pyrazolyl signals due to the fluxional motion.
15 (*a*) A. W. Addison, T. N. Rao, J. Reedijk, J. van Rijn and G. C. Verschoor, *J. Chem. Soc., Dalton Trans.*, 1984, 1349; see also; (*b*) S. Alvarez and M. Llunell, *J. Chem. Soc., Dalton Trans.*, 2000, 3288.
16 M. B. Smith and J. March, *Advanced Organic Chemistry*, Wiley Interscience, New York, 5th edn., 2001.
17 Large B_{eq} values are noted for some of the isopropenyl groups suggesting occurrence of disorder problems, which may arise from (1) two orientations of the isopropenyl group, (2) disorder with a non-dehydrogenated isopropyl group, and (3) a combination of (1) and (2). For example, the cell parameters for the dehydrogenated nickel complex **5b(Ni)** and the non-dehydrogenated cobalt complex **6b(Co)** were virtually the same suggesting occurrence of dehydrogenation for the cobalt complex. The thermal parameters for the part corresponding to the dehydrogenation site (C64–66) were large and some disorder was evident. We tried refinements taking into account the three possibilities. However, the attempts were unsuccessful and the disordered atoms could not be resolved sufficiently, indicating that occurrence of the dehydrogenation could not be determined by the crystallography alone. Then taking into account the results of the spectroscopic data, in particular, the FD-MS data, complexes **5b(Ni)** and **6b(Co)** were refined as the dehydrogenated and non-dehydrogenated form, respectively. As a result, the meaningful difference in the structural parameters, enough to support the dehydrogenation process was noted, although the structural parameters come from averaged structures. The structural parameters for C64–66 of **6b(Co)** are as follows: C64–C65: 1.44(2) Å; C64–C65: 1.44(3) Å; $\alpha + \beta + \gamma = 338°$. The deviation from planarity of the central carbon atom (C64) clearly indicated its sp^3-hybridization.
18 O. M. Reinaud and K. H. Theopold, *J. Am. Chem. Soc.*, 1994, **116**, 6979; in this study, the primary product was not isolated but the isopropenylpyrazole obtained after acidic work-up was characterized. Although it was evident that some oxidation process occurred, it was impossible to discriminate the dehydrogenation from alternative routes including dehydration of the 1-hydroxy-1-methyl-ethyl group [–CMe_2(OH)] formed by oxygenation of the methine carbon atom.
19 Complex **2** is stable at room temperature.
20 T. Higashi, Program for absorption correction, Rigaku Corp., Tokyo, Japan, 1995.
21 teXsan; Crystal Structure Analysis Package, ver. 1. 11, Rigaku Corp., Tokyo, Japan, 2000.
22 International Tables for X-ray Crystallography, Kynoch Press, Birmingham, 1975, **vol. 4**.
23 (*a*) G. M. Sheldrick, SHELXS-86: Program for crystal structure determination, University of Göttingen, Göttingen, Germany, 1986; (*b*) G. M. Sheldrick, SHELXL-97: Program for crystal structure refinement, University of Göttingen: Göttingen, Germany, 1997.
24 P. T. Beurskens, G. Admiraal, G. Beurskens, W. P. Bosman, S. Garcia-Granda, R. O. Gould, J. M. M. Smits and C. Smykalla, The DIRDIF program system, Technical Report of the Crystallography Laboratory, University of Nijmegen, Nijmegen, The Netherlands, 1992.